J. Fluid Mech. (2009), *vol.* 640, *pp.* 187–214.
doi:10.1017/S0022112009991315

Transcritical shallow-water flow past topography: finite-amplitude theory

G. A. EL[1]†, R. H. J. GRIMSHAW[1] AND N. F. SMYTH[2]

[1]Department of Mathematical Sciences, Loughborough University, Loughborough LE11 3TU, UK

[2]School of Mathematics and Maxwell Institute for Mathematical Sciences, University of Edinburgh, The King's Buildings, Mayfield Road, Edinburgh, Scotland EH9 3JZ, UK

(Received 24 March 2009; revised 21 July 2009; accepted 21 July 2009; first published online 4 November 2009)

We consider shallow-water flow past a broad bottom ridge, localized in the flow direction, using the framework of the forced Su–Gardner (SG) system of equations, with a primary focus on the transcritical regime when the Froude number of the oncoming flow is close to unity. These equations are an asymptotic long-wave approximation of the full Euler system, obtained without a simultaneous expansion in the wave amplitude, and hence are expected to be superior to the usual weakly nonlinear Boussinesq-type models in reproducing the quantitative features of fully nonlinear shallow-water flows. A combination of the local transcritical hydraulic solution over the localized topography, which produces upstream and downstream hydraulic jumps, and unsteady undular bore solutions describing the resolution of these hydraulic jumps, is used to describe various flow regimes depending on the combination of the topography height and the Froude number. We take advantage of the recently developed modulation theory of SG undular bores to derive the main parameters of transcritical fully nonlinear shallow-water flow, such as the leading solitary wave amplitudes for the upstream and downstream undular bores, the speeds of the undular bores edges and the drag force. Our results confirm that most of the features of the previously developed description in the framework of the unidirectional forced Korteweg–de Vries (KdV) model hold up qualitatively for finite amplitude waves, while the quantitative description can be obtained in the framework of the bidirectional forced SG system. Our analytic solutions agree with numerical simulations of the forced SG equations within the range of applicability of these equations.

1. Introduction

Description of shallow-water flow over an obstacle is a classical and fundamental problem in fluid mechanics, with implications for flow interaction with topography in many other physical contexts. Our concern here is with the upstream and downstream waves that may be generated for flow over a one-dimensional localized obstacle, that is, the obstacle is uniform in the direction transverse to the oncoming flow, and is localized in the flow direction. When the flow is not critical, that is, when the Froude number $F = V/c$ is not close to unity, where V is the oncoming flow speed and $c = (gh)^{1/2}$ is the linear long-wave speed in water of undisturbed depth h, linear theory

† Email address for correspondence: G.El@lboro.ac.uk

may be used to describe the wave field. For subcritical flow ($F < 1$) stationary lee waves are found downstream, together with transients propagating both upstream and downstream, while only downstream-propagating transients are found in supercritical flow ($F > 1$). However, these linear solutions fail near criticality ($F = 1$), as then the wave energy cannot propagate away from the obstacle. In this case it is necessary to invoke nonlinearity to obtain a suitable theory, and it is now well established that the forced Korteweg–de Vries (fKdV) equation is an appropriate model for the *weakly nonlinear* regime (see for instance Grimshaw, Zhang & Chow 2007 and the references therein).

The structure of the transcritical (or resonant) flows over localized topography modelled by the fKdV equation is now well understood. Combinations of the locally steady hydraulic solution, with its associated upstream and downstream hydraulic jumps, and the modulation solutions describing upstream and downstream undular bores which resolve these jumps, obtained by Grimshaw & Smyth (1986) and Smyth (1987), showed excellent agreement with direct numerical simulations of the fKdV equation. On the other hand, a recent comparison in Grimshaw *et al.* (2007) of fKdV dynamics with the corresponding numerical solution of the full Euler equations for transcritical flow showed that, while the fKdV model successfully reproduces essential qualitative features of the flow, quantitative differences could be quite significant for large obstacles. In this paper, we address this issue by seeking analytical and numerical solutions of the Su–Gardner (SG) equations, derived by Su & Gardner (1969) to describe fully nonlinear water waves in the long-wave regime.

The SG system has the typical structure of the well-known Boussinesq-type systems for shallow water waves, but differs from them in retaining full nonlinearity in the leading-order dispersive term. Thus it is expected to be superior to traditional weakly nonlinear Boussinesq models in reproducing quantitative features of fully nonlinear dispersive flows.

Other fully nonlinear shallow water models exist which retain higher order dispersive terms and describe the behaviour of finite amplitude waves better than the SG equations (see for instance Gobbi, Kirby & Wei 2000 and Madsen, Bingham & Schäffer 2003 and references therein). These models, however, are typically far more complicated than the SG system and do not possess its degree of universality in terms of applicability in other fluid dynamics contexts, such as bubbly fluid dynamics Gavrilyuk (1994) and dispersive magnetohydrodynamics Dellar (2003). Our aim in this paper is to construct an *analytical* theory of shallow-water irrotational transcritical flows, this being presently available only for the weakly nonlinear case modelled by the fKdV equation. So the choice of the SG system as the closest to the KdV equation, in terms of complexity, and as a fully nonlinear bidirectional model is natural. We also note that detailed numerical comparisons by Ertekin, Webster & Wehausen (1986) and Nadiga, Margolin & Smolarkiewicz (1996) showed that the SG equations reproduce the finite-amplitude Euler equation dynamics of flow past topography, excluding any possible effects of wave breaking.

The description of an undular bore generated by an initial step was first constructed by Gurevich & Pitaevskii (1974) in the framework of the Korteweg–de Vries (KdV) equation, using the Whitham modulation theory (see Whitham 1974). This solution was used by Grimshaw & Smyth (1986) and Smyth (1987) to describe the generation of upstream and downstream undular bores generated by transcritical flow over topography in the framework of the fKdV equation. In that case, explicit analytic solutions could be found, as for the KdV equation Riemann invariants are available for the associated modulation system, which in turn is a consequence of the integrability of the KdV equation. The SG system is not integrable and the Riemann invariants

for its modulation system are not available. A method for the analysis of the undular bores which does not require the existence of the Riemann invariant form of the modulation system was developed by El (2005) (see also El, Khodorovskii & Tyurina 2005). This method was applied to the SG system by El, Grimshaw & Smyth (2006) where the main parameters of the so-called simple undular bores were derived. In this present paper we use this theory to study the generation of finite-amplitude undular bores generated by transcritical shallow-water flow past a localized obstacle in the framework of the forced SG equations. Our main aim is to obtain the dependence of the parameters defining the undular bores, such as the leading soliton amplitude and the speeds of the undular bore edges, on the magnitude of the topographic forcing and the Froude number of the oncoming flow.

Thus we consider one-dimensional shallow-water flow past topography. The flow can be described by the total local depth H and the depth-averaged horizontal velocity U. The basic equations are derived in the Appendix, and are just the usual SG equations, but modified by the forcing term due to localized topographic obstacle $f(x)$ defined so that the bottom is located at $z=-h+f(x)$ where h is the undisturbed depth at infinity. Here we shall use non-dimensional coordinates, based on a length scale h, a velocity scale $\sqrt{gh}$ and a time scale of $\sqrt{h/g}$. Then the forced SG equations are

$$\zeta_t + (HU)_x = 0, \quad H = 1 + \zeta - f, \tag{1.1}$$

$$U_t + UU_x + \zeta_x = -\frac{(H^2D^2H)_x}{3H} - \frac{(H^2D^2f)_x}{2H} - \frac{f_xD^2(\zeta+f)}{2}, \tag{1.2}$$

where

$$D = \frac{\partial}{\partial t} + U\frac{\partial}{\partial x}.$$

This agrees with the original SG system when $f=0$. When $f \neq 0$ the only difference lies in the nonlinear dispersive terms in (1.2).

The forced SG system (1.1) and (1.2), in spite of its rather complicated form, is much more amenable to analytical treatment than the full Euler equations. First, it has well defined hyperbolic, dispersive and forcing components, so that the construction of the hydraulic solution is possible. Second, as will be found later, undular bores are formed away from the topographic forcing itself, so one can take advantage of the modulation theory available for the unforced, standard SG system. Such a modulation theory is, however, not available for the full Euler equations.

We note that the much discussed issue of the varying vorticity in the two-dimensional (x, y, t) version of the SG equations, conventionally called the Green–Naghdi equations (Green & Naghdi 1976) (see for instance Miles & Salmon 1985 and Kim *et al.* 2001), does not arise in the present effectively one-dimensional (x, t) scenario. We also add that in the present work we consider laminar undular bores, so that the large amplitude effects of wave breaking, implying rotational flows in the (x, z) plane, are beyond the scope of the present paper.

We shall suppose that the upstream flow is the constant horizontal velocity $V>0$, in dimensional coordinates, which becomes $F=V/\sqrt{gh}$, the Froude number, in the non-dimensional coordinate system. Since we are considering a localized obstacle, we require that $f=0$ for $|x|>L$ say, and $f>0$ when $|x|<L$ with a maximum of f_m at $x=0$. Then our asymptotic solution procedure assumes that that $L \gg 1$, and so in $|x|<L$ we can use a hydraulic approximation to obtain subcritical, supercritical and transcritical solutions, analogous to those described by Grimshaw & Smyth (1986) for the fKdV equation, and by Baines (1995) for fully nonlinear and non-dispersive

flow. In the transcritical regime these solutions form upstream and downstream discontinuities relative to the undisturbed flow at infinity, that is, hydraulic jumps. These discontinuities are resolved by the insertion of undular bores and since in $|x| > L$ we have the homogeneous SG equations, the Whitham modulation theory (Whitham 1974) can be applied there.

An important development outlined in this paper compared with previous studies is that we derive the closure conditions for the transcritical hydraulic solution of the forced shallow water equations based on an undular bore resolution and show that, for weak to moderate values of the forcing, the downstream rarefraction wave predicted by general hydrodynamic reasoning (see Baines 1995 for instance) has a very small amplitude and can be neglected for any practical purpose. The absence, or, to be precise, negligibly small amplitude of the downstream rarefraction wave is confirmed by our numerical simulations of the SG equations and is also a feature of the full Euler equations (see Grimshaw *et al.* 2007). This has the important implication that the problem of transcritical shallow water flow past topography is essentially unidirectional, which, in particular, formally justifies the applicability of the unidirectional fKdV equation in the description of weakly nonlinear transcritical flows in Grimshaw & Smyth (1986).

In the remainder of this paper, we present the hydraulic solutions in § 2, and the required undular bore solutions in § 3. We conclude with a discussion in § 4.

2. Hydraulic approximation

We shall follow the approach of Grimshaw & Smyth (1986), the key point of which is the assumption, confirmed by direct numerical simulations, of the existence, in the transcritical regime, of a locally steady hydraulic transition in the forcing region. This is characterized by a subcritical constant elevation $\zeta^- > 0$ and velocity $U < F$ upstream and a supercritical constant depression $\zeta^+ < 0$ and velocity $U > F$ downstream. These states are resolved back to the equilibrium state $\zeta = 0$, $U = F$ by two undular bores, propagating upstream and downstream respectively. Apart from the account of the large-amplitude effects, the qualitative difference between the KdV case studied in Grimshaw & Smyth (1986) and the present case of the SG system is that now we deal with the equations describing bidirectional wave propagation so the mentioned combination of just two undular bores may generally be not sufficient to resolve the upstream and downstream discontinuities in depth and velocity.

First, we need to determine the upstream elevation and velocity at $x = -L$ and the downstream depression and elevation at $x = L$. As in Grimshaw & Smyth (1986), this can be done by using the hydraulic approximation, in which the dispersive term in (1.2) is omitted, and we then seek steady solutions of the remaining equations which, relative to the oncoming flow F, have a subcritical elevation upstream and a supercritical depression downstream. These steady hydraulic equations are

$$HU = (1 + \zeta - f)U = Q, \quad \zeta + \frac{U^2}{2} = B. \tag{2.1}$$

Here Q, B are positive integration constants, representing mass and energy respectively (strictly B is the Bernoulli constant and BQ is energy). Eliminating ζ gives

$$\frac{U^2}{2} + \frac{Q}{U} = B + 1 - f, \tag{2.2}$$

which determines U as a function of the obstacle height f.

For non-critical flow, the solution (U, ζ) of (2.1), (2.2) must tend to $(F, 0)$ at infinity, and so $Q = F$, $B = F^2/2$. In terms of the upstream Froude number it is then required that (see for instance Baines 1995)

$$0 < f_m < 1 + \frac{F^2}{2} - \frac{3F^{2/3}}{2}. \tag{2.3}$$

This expression defines the subcritical regime $F < F_- < 1$ and the supercritical regime $1 < F_+ < F$ where a smooth steady hydraulic solution exists. For small $f_m \ll 1$, we find that

$$F_\pm = 1 \pm \sqrt{\frac{3f_m}{2}}. \tag{2.4}$$

In the transcritical regime $F_- < F < F_+$ where (2.3) does not hold, we seek instead a solution that has upstream and downstream jumps, and which satisfies the critical flow condition at the top of the obstacle. That is we require that when $f_x = 0$ at $x = 0$, $U_x \neq 0$. This condition leads to

$$U(x = 0) = U_m = Q^{1/3}. \tag{2.5}$$

Note that we can define a local Froude number Fr by

$$(Fr)^2 = \frac{U^2}{H} = \frac{U^3}{Q} = \frac{U^3}{U_m^3}, \quad \text{and so} \quad Fr = 1 \text{ at } x = 0. \tag{2.6}$$

Later it will emerge that there is subcritical flow upstream ($Fr < 1, U < U_m, x < 0$) and supercritical flow downstream ($Fr > 1, U > U_m, x > 0$). Evaluating (2.2) at $x = 0$ we get

$$\frac{3U_m^2}{2} = \frac{3Q^{2/3}}{2} = B + 1 - f_m. \tag{2.7}$$

For a given obstacle height, this relation defines B in terms of Q. Also we note that the elevation $\zeta(x = 0) = \zeta_m$ at the top of the obstacle is given by

$$\zeta_m = B - \frac{U_m^2}{2}. \tag{2.8}$$

It follows that $\zeta > \zeta_m, U < U_m$ upstream, and $\zeta < \zeta_m, U > U_m$ downstream.

Next outside the obstacle in $U = U_\pm, \zeta = \zeta_\pm$ are constant, downstream ($x > L$) and upstream ($x < -L$) respectively. We must now determine how these constants are related to the undisturbed values $U = V, \zeta = 0$ far downstream and upstream. This will depend on whether the adjustment is through a classical (frictional) shock, or through an undular bore. Before proceeding we note the relationships

$$U_\pm(1 + \zeta_\pm) = Q, \tag{2.9}$$

$$\frac{U_\pm^2}{2} + \zeta_\pm = B, \tag{2.10}$$

$$\text{and so} \quad \frac{U_\pm^2}{2} + \frac{Q}{U_\pm} = \frac{Q^2}{2(1 + \zeta_\pm)^2} + \zeta_\pm + 1 = B + 1. \tag{2.11}$$

For given Q, B, these relations fix $U_\pm, \zeta_\pm$ completely, provided we can establish that the required solution must have $U_+ > U_-, \zeta_+ < \zeta_-$. But we have one relationship (2.7) connecting B, Q, and so there is just a single constant to determine. Also note that

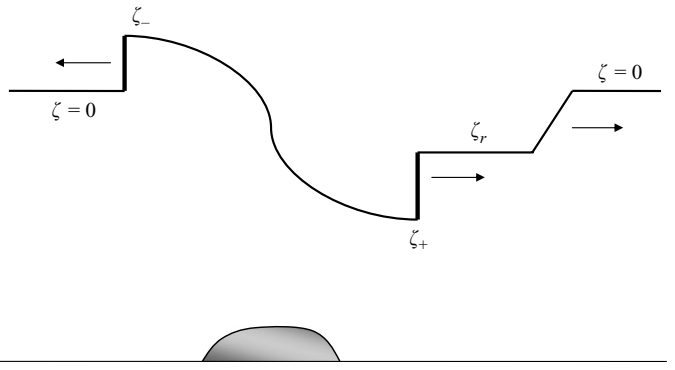

FIGURE 1. Schematic for closure using classical shocks. The shaded area shows the position of the bottom ridge.

the respective criteria that $\zeta_\pm = 0$ recover the boundaries of the transcritical regime defined by equality in (2.19).

2.1. *Classical shock closure*

We follow first the classical approach and consider downstream and upstream jump resolution by classical shocks. Apart from being methodologically instructive this consideration is relevant to the case of large-amplitude topography that would generate classical turbulent bores.

If S is the shock speed, and $[\cdots]$ denotes a jump, the classical shocks conserve mass and momentum, and so we get, in $|x| > L$,

$$-S[\zeta] + [HU] = 0, \quad -S[HU] + \left[HU^2 + \zeta + \frac{1}{2}\zeta^2\right] = 0. \tag{2.12}$$

Note the steady flow over the obstacle conserves mass and energy (rather than momentum) so these are non-trivial conditions to apply. However, we cannot simultaneously impose upstream and downstream jumps which connect directly to the uniform flow. Instead, we follow Baines (1995), and first impose an upstream jump. There is then a downstream jump which connects to a rarefraction wave (see figure 1). First, we consider the upstream jump, which connects ζ_-, U_- to 0, F with $S_- < 0$, S_- being the speed of the upstream shock. The first relation in (2.12) gives

$$\zeta_-(S_- - F) = (1 + \zeta_-)(U_- - F), \quad \text{or} \quad \zeta_-(S_- - U_-) = U_- - F. \tag{2.13}$$

But then, using the relations (2.9) we also get

$$S_-\zeta_- = Q - F. \tag{2.14}$$

Next, the second relation in (2.12) gives

$$(1 + \zeta_-)(U_- - F)(S_- - U_-) = \zeta_-\left(1 + \frac{\zeta_-}{2}\right). \tag{2.15}$$

Eliminating S_- gives

$$(1 + \zeta_-)(U_- - F)^2 = \zeta_-^2\left(1 + \frac{\zeta_-}{2}\right), \tag{2.16}$$

while eliminating $U_- - F$ gives

$$(S_- - F)^2 = (1+\zeta_-)\left(1+\frac{\zeta_-}{2}\right), \tag{2.17}$$

$$\text{so that} \quad S_- = F - \left[(1+\zeta_-)\left(1+\frac{\zeta_-}{2}\right)\right]^{1/2}. \tag{2.18}$$

Here the choice of sign is dictated by the requirement that this solution is to hold in the transcritical regime. Further, since we need $S_- < 0$ it follows that we must have $\zeta_- > 0$. Then the relations (2.9), (2.14) show that also $U_- < Q < F$.

The system of equations is now closed, as substitution of (2.18) into (2.14) determines ζ_- in terms of Q, and then we can use (2.11) to determine Q in terms of B, so that finally all unknowns are obtained in terms of f_m from (2.7). Further, the conditions $\zeta_- > 0$ serve to define the transcritical regime in terms of the Froude number F and f_m,

$$f_m > 1 + \frac{F^2}{2} - \frac{3F^{2/3}}{2}. \tag{2.19}$$

This of course is precisely the opposite of the condition (2.3) for non-critical flow. In the weakly nonlinear limit, this procedure yields

$$\zeta_\pm = \frac{2}{3}(F-1) \mp \sqrt{\frac{2f_m}{3}}, \tag{2.20}$$

which holds in the transcritical regime $|F-1| < (3f_m/2)^{1/2}$.

This procedure also determines $\zeta_+ < 0$, $U_+ > U_m$, but in general, these cannot be resolved by a jump directly to the state 0, F. Instead we must insert a right-propagating rarefraction wave, as in Baines (1995) (see figure 1). The rarefraction wave propagates downstream into the undisturbed state 0, F, and so is defined by the values ζ_r, U_r where

$$U_r - 2(1+\zeta_r)^{1/2} = F - 2. \tag{2.21}$$

The rarefraction wave is then connected to the 'hydraulic' downstream state near topography ζ_+, U_+ by a shock, using the jump conditions (2.12) to connect the two states through a shock with speed $S_+ > 0$. There are then three equations for the three unknowns ζ_r, U_r, S_+ and the system is closed.

Note that in the weakly nonlinear regime, when the forcing is sufficiently small (the appropriate small parameter is $\epsilon \sim \sqrt{f_m}$), the rarefraction wave contribution can be neglected as it has the amplitude of order ϵ^3 while the shock intensity is $O(\epsilon)$ (see the next section).

2.2. *Undular bore closure*

Now suppose that instead we use undular bores to resolve the shocks. Then upstream we must impose the condition for a simple undular bore (see El *et al.* 2006), while downstream we should in principle allow for a rarefraction wave in addition to another simple undular bore (see figure 2). The simple undular bore transition condition requires that one of the Riemann invariants of the ideal shallow-water equations (the dispersionless limit of the system (1.1), (1.2) with a zero right-hand side) should have a zero jump across the bore. The choice of the Riemann invariant is suggested by the comparison with the well-understood weakly nonlinear theory (Grimshaw & Smyth 1986 and Smyth 1987). Indeed, in the weakly nonlinear approximation for transcritical flow past topography both the upstream and the downstream undular bores are

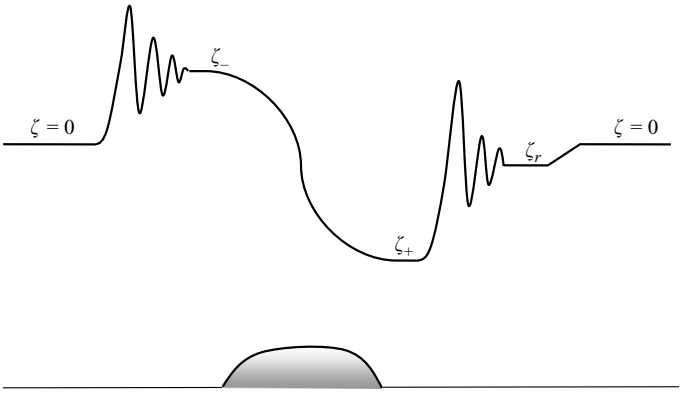

FIGURE 2. Schematic for closure using undular bores. The shaded area shows the position of the bottom ridge.

modelled within the framework of the same left-propagating forced KdV equation. This implies that for the forced SG system the appropriate left-propagating simple undular bore conditions should be applied to both the upstream and downstream flow.

Thus for the upstream undular bore we have

$$U_- + 2(1+\zeta_-)^{1/2} = F + 2, \tag{2.22}$$

or, equivalently, using (2.9),

$$\frac{Q}{1+\zeta_-} + 2(1+\zeta_-)^{1/2} = U_- + \frac{2Q^{1/2}}{U_-^{1/2}} = F + 2. \tag{2.23}$$

This expression then replaces (2.13), (2.18), and in conjunction with (2.11) determines ζ_-, U_-, Q in terms of F, f_m. As for the classical shock closure, the condition $\zeta_- > 0$ again defines the transcritical regime by (2.19). Note that the expression (2.23) can be expanded in powers of ζ_- to yield

$$Q = F + (F-1)\zeta_- - \frac{3\zeta_-^2}{4} + \frac{\zeta_-^3}{8} + \cdots. \tag{2.24}$$

This agrees with the corresponding expression obtained from the classical shock closure using (2.13) up to the second-order term, while the third-order term is then $\zeta_-^3/16$. Since the final determination of ζ_- in terms of F, f_m is then given by (2.11) in both cases, it follows that these results will also agree up to the second-order terms in ζ_-, where we note that $F-1 \sim \zeta_-$ for transcritical flow. A plot of f_m in terms of ζ_- for $F=1$ is shown in figure 3, where we also show the corresponding result using the classical shock closure. We see that ζ_- is slightly smaller when using the undular bore closure than for the classical shock closure, but is indeed quite close over the whole range of f_m. However, while the closure conditions for classical and undular bores are very close, their structure and speeds of propagation are drastically different. Indeed, in contrast to the classical shock, the undular bore expands with time and is characterized by two speeds, the leading edge propagating with the soliton speed and the trailing with the linear group velocity. Both speeds are different from the classical shock speed. For instance, for the KdV equation $u_t + uu_x + u_{xxx} = 0$ the corresponding classical shock speed (found from the dispersionless 'mass' balance $u_t + (u^2/2)_x = 0$) is $s = \Delta/2$, where $\Delta = u_- - u_+$ is the jump across the shock, while for

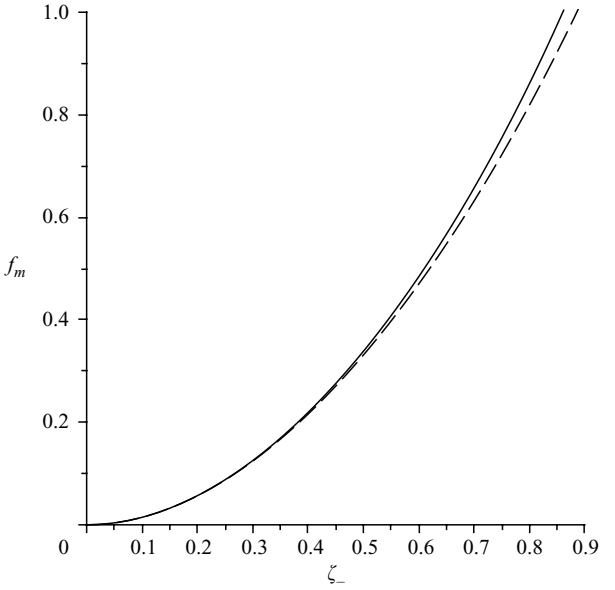

FIGURE 3. Plot of ζ_- as a function of f_m for $F=1$; the solid line is the classical shock closure and the dashed line is the undular bore closure.

the undular bore with the same jump Δ the leading edge propagates with the velocity $s_+ = 2\Delta/3$ and the trailing edge with the velocity $s_- = -\Delta$ (see Gurevich & Pitaevskii 1974 and Fornberg & Whitham 1978). The speeds of the upstream and downstream undular bore edges for the forced SG system will be determined in terms of f_m, F in the subsequent sections. Also, we note that from the analytical point of view it is essential that we use the undular bore closure condition (2.22) rather than classical shock closure (2.16) as condition (2.22) is consistent with the Whitham modulation equations describing slow variations of the travelling wave parameters in the undular bore (see El 2005 and El *et al.* 2005).

As for the classical shock closure, the downstream undular bore can now be found independently of the upstream state, where we would generally use

$$U_+ + 2(1+\zeta_+))^{1/2} = U_r + 2(1+\zeta_r)^{1/2}, \tag{2.25}$$

where U_r, ζ_r are the parameters of an additional intermediate constant state which is connected to the unperturbed flow $U=F, \zeta=0$ through a right-propagating rarefraction wave satisfying the transition condition (2.21). This analysis can be simplified by noticing that for sufficiently small values of topographic forcing one can neglect the contribution of the rarefraction wave into the solution and connect the downstream undular bore directly to the undisturbed flow $U=F$, $\zeta=0$. To show this, we consider the jump of the Riemann invariant of the unforced ideal shallow-water equations, $U + 2(1+\zeta)^{1/2}$, defining the simple undular bore transition, across the transcritical hydraulic solution. For that, using (2.5), (2.9), we introduce dimensionless quantities $v_\pm = U_\pm/U_m$ to transform (2.11) into

$$v_\pm^2 + \frac{2}{v_\pm} - 3 = \alpha, \tag{2.26}$$

where $\alpha = 2f_m/U_m^2$. For small values of the topographic forcing, when $\alpha \ll 1$, we expect $v_\pm 1$. Then from (2.26) we get the expansion

$$v_\pm = 1 \pm \left(\frac{\alpha}{3}\right)^{1/2} + \frac{\alpha}{9} + c_\pm \alpha^{3/2} + \cdots . \tag{2.27}$$

The coefficients $c_\pm$ in (2.27) will not contribute to the result so we do not present them explicitly. Next we consider the quantities

$$\Lambda_\pm = \frac{1}{U_m}\left(U_\pm + \frac{2Q^{1/2}}{U_\pm^{1/2}}\right) = v_\pm + \frac{2}{v_\pm^{1/2}}, \tag{2.28}$$

which are just the normalized Riemann invariants (2.25) and (2.22) defining the downstream and upstream undular bore transitions respectively. Expanding (2.28) for small α we get that

$$\Lambda_\pm = 3 + \frac{\alpha}{4} \mp \frac{\alpha^{3/2}}{24\sqrt{3}} \cdots . \tag{2.29}$$

Now, taking into account that for weak topography $U_m = 1$ to leading order, we get that

$$\Lambda_- - \Lambda_+ = 2\left(\frac{f_m}{6}\right)^{3/2} + \cdots . \tag{2.30}$$

Thus for small topographic forcing the Riemann invariant controlling the undular bore transition condition has a jump of only the third order in the small parameter $\sqrt{f_m}$ across the forcing region. It is not difficult to show now that the magnitude $\Delta\zeta$ of the downstream rarefraction wave forming due to this small jump of the Riemann invariant across the forcing region to leading order is $\Delta\zeta \approx (\Lambda_- - \Lambda_+)/2 \approx (f_m/6)^{3/2}$. This implies that one can neglect the downstream rarefraction wave and use the same transition condition (2.22) for the downstream undular bore. That is, henceforth we can assume that

$$U_- + 2(1+\zeta_-)^{1/2} = U_+ + 2(1+\zeta_+)^{1/2} = F + 2. \tag{2.31}$$

Of course, it is well known that in the case of weak topography the resonant flow problem is modelled by the unidirectional forced KdV equation (see for instance Grimshaw & Smyth 1986) so that the simple-wave relationship (2.31) is already taken into account in this model. In this respect, the result (2.31) for weak topography is to be expected and can be regarded as a formal justification of the validity of the unidirectional KdV approximation in the modelling of the resonant flow past topography. On the other hand, relationship (2.30) shows that within the range of applicability of the SG model one can consistently neglect the downstream rarefraction wave and at the same time capture effects $O(\sqrt{f_m})$ which could be well beyond the KdV approximation.

Now, having the full hydraulic solution for the transcritical region (2.3), we use (2.7), (2.9), (2.10), (2.11), (2.31) to plot the values of the upstream and downstream elevation (depression) jumps, ζ_- and ζ_+ as functions of the topography amplitude f_m for a fixed value of the Froude number say $F = 1$ and as functions of the Froude number F for a fixed value of f_m (we take $f_m = 0.2$). The corresponding plots are presented in figure 4. One can see that at the lower boundary $F_- \approx 0.47$ of the transcritical regime one has a downstream bifurcation (ζ^+ 'switches' from 0 to about -0.6) while at the upper boundary $F_+ \approx 1.56$ there is an upstream bifurcation from $\zeta_- = 0$ to about 0.9.

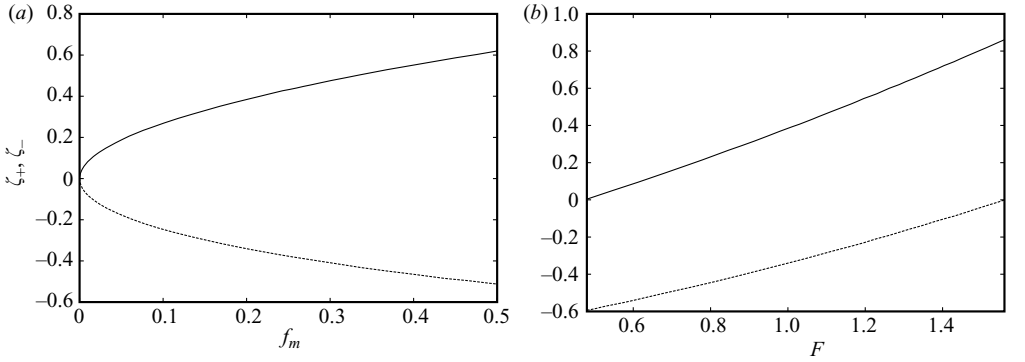

FIGURE 4. Upstream elevation ζ_- (solid line) and downstream depression ζ_+ (broken line) as functions of the topography strength f_m for fixed Froude number $F = 1$ (a) and the Froude number F for fixed $f_m = 0.2$ (b) in the local hydraulic transcritical solution.

It is clear that for flows with Froude numbers close to the transcritical region boundaries $F_\pm$ our assumption about the existence of a steady hydraulic transition over the topographic forcing might not be valid as it assumes that the time for the establishment of this transition is much less than that for the formation of the developed wave structure of the undular bore. Indeed, our numerical simulations with the Froude numbers close to the values $F_\pm$ show that the steady hydraulic flow over the topography does not establish itself within the simulation time. So one can expect noticeable departures of the actual details of the flow from the analytic predictions based on the above assumption.

Thus, near the transcritical region boundaries an additional (non-stationary) analysis is required to clarify validity of the local hydraulic solution in the global description of the transcritical flow. Such an analysis is beyond the scope of the present paper, instead, we shall simply compare our analytic results with direct numerical solutions of the forced SG system.

3. Downstream and upstream undular bore resolution

3.1. *Numerical solution*

In the subsequent subsections, we shall derive analytically the main parameters of the undular bores generated in transcritical shallow-water flow past a localized obstacle modelled by the forced SG equations (1.1), (1.2). These will be compared with the results of direct numerical simulations of the system (1.1), (1.2).

The numerical scheme was developed using centred differences in space and time, so that the error was $O(\Delta x^2, \Delta t^2)$, where Δx and Δt are the space and time steps respectively. More precisely, the mass conservation equation (1.1) was solved using the Lax–Wendroff method, which is an explicit method and has second-order accuracy in Δt and Δx. The momentum equation (1.2) was solved using centred differences in x and t for the derivatives, which resulted in an implicit scheme which required solving a tridiagonal system at each time step, which is numerically fast. This implicit scheme was also second-order accurate in Δt and Δx. The combined hybrid scheme was found to be stable, for sufficiently small Δt. For the numerical simulations we used the choice $f(x) = f_m \exp(-x^2/w^2)$ with $w = 8$ for the forcing term.

It will be shown that for weak topographies our theory reproduces the analytical results obtained (and verified numerically) earlier in the framework of the forced

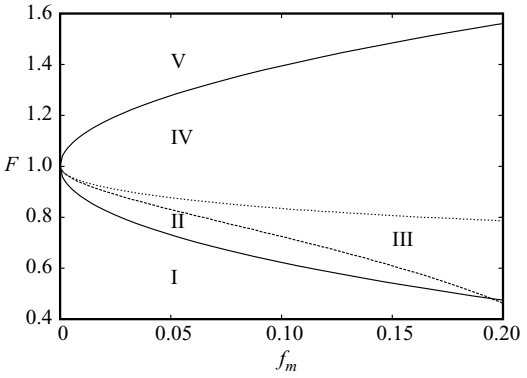

FIGURE 5. The regions of the f_m, F plane corresponding to different configurations of the flow past topography. Solid line: the transcritical region boundaries $F_+ > F_-$ defined by the equality in (2.3). For $F < F_-$ (region I) and $F > F_+$ (region V) one has the hydraulic flow smoothly connecting to $\zeta = 0, U = F$ at infinity; in the regions II–IV undular bores are generated. Region II corresponds to the attached downstream undular bore and detached upstream undular bore; in the region III both undular bores are detached; in the region IV there is an attached upstream bore (soliton train) and a detached downstream bore.

KdV equation. Therefore, in the numerical comparisons we shall concentrate on the finite-amplitude waves and will test the obtained analytical solutions for a broad range of amplitudes performing the simulations even outside the range of formal applicability of the SG model to actual shallow-water flows.

In the forced KdV dynamics with broad localized forcing one of the undular bores is always attached to the topography while another one is fully realized. Which bore (upstream or downstream one) is attached is determined by the actual combination of the forcing amplitude f_m and the Froude number F of the oncoming flow. The 'switchover' between two attached bores occurs on a certain line in the (f_m, F) plane. As we shall show, in the fully nonlinear SG theory this 'switchover' line splits into a domain corresponding to the configuration with both undular bores fully realized and completely detached from the topography. The diagram showing different regions of the (f_m, F) plane is presented in figure 5. The equations of the transcritical region boundaries $F_+ > F_-$ are given by the equality in (2.3). The equations for the internal boundaries separating regions II, III and IV will be derived later.

In figure 6 two numerical solutions for the surface displacement ζ in the forced SG system (1.1), (1.2) are shown for the input parameters corresponding to the regions IV and II of figure 5. Further, in figure 7 the numerical solution corresponding to the region III with two completely detached bores is presented. One can see that the numerical solutions confirm our main assumption about the existence, in the topography forcing region, of the steady hydraulic transcritical solution forming downstream and upstream jumps which are further resolved back into the undisturbed flow via undular bores. Another important feature of the numerical solution confirming our theory so far is the fact that the downstream large-amplitude undular bore resolves (almost) directly back into the undisturbed flow without the need of a further rarefraction wave which could be there from general reasoning described in § 2. A very small departure of the equilibrium state downstream of the bore from the undisturbed flow with $\zeta = 0$, which can be seen in both figures, agrees with our prediction in § 2.2, which gives $\Delta\zeta \approx (f_m/6)^{3/2} \sim 10^{-3}$ (i.e. about 1 %–2 % of the depth jump across the downstream undular bore for the forcing amplitudes used

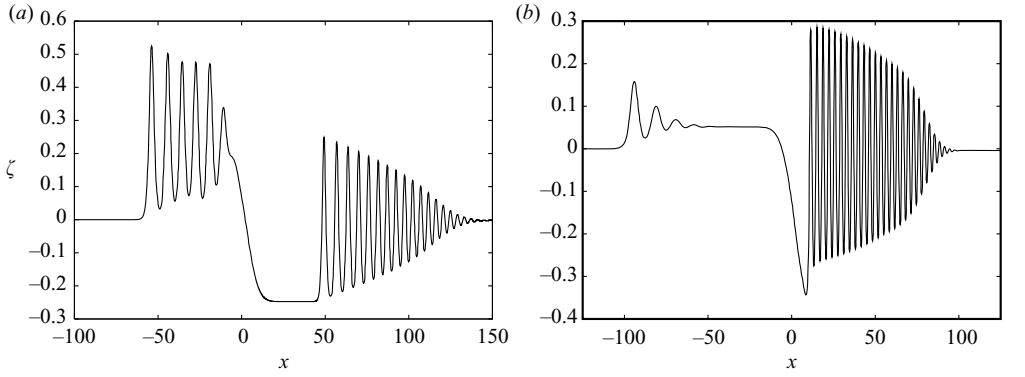

FIGURE 6. Undular bore resolution in the transcritical flow past broad topography. (*a*) Attached upstream bore and detached downstream bore ($f_m = 0.1$, $F = 1$, $t = 250$) (region IV in figure 5); (*b*) attached downstream and detached upstream bore ($f_m = 0.1$, $F = 0.7$, $t = 250$) (region II).

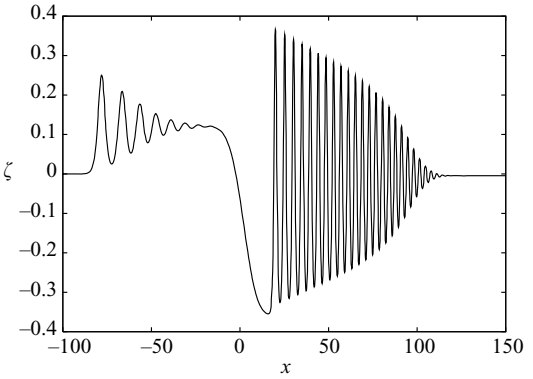

FIGURE 7. Undular bore resolution in the transcritical flow past broad topography ($f_m = 0.1$, $F = 0.8$, $t = 250$): both bores are detached (region III).

in our simulations). Thus the contribution of the corresponding rarefraction wave can indeed be neglected for any practical purpose.

3.2. *General analytic construction*

Based on the results of our numerical simulations we shall assume that the downstream and upstream undular bores are generated outside the region of the topographic forcing. Therefore we can take advantage of the modulation theory of undular bores in the standard, unforced SG equations developed in El *et al.* (2006) and El, Grimshaw & Smyth (2008). To be consistent with the notations of the aforementioned papers we introduce $\eta = 1 + \zeta$, $u = U$ and represent the unforced SG system in the form

$$\eta_t + (\eta u)_x = 0, \tag{3.1}$$

$$u_t + u u_x + \eta_x = \frac{1}{\eta}\left[\frac{1}{3}\eta^3(u_{xt} + u u_{xx} - (u_x)^2)\right]_x .$$

Now we explicitly present the upstream and downstream hydraulic states for the transcritical regime, $F_- < F < F_+$

$$\text{at} \quad x = -L: \qquad \eta = \eta_u > 1, \quad u = u_u < F, \tag{3.2}$$

$$\text{at} \quad x = L: \qquad \eta = \eta_d < 1, \quad u = u_d > F, \tag{3.3}$$

$$\text{where} \quad \eta_d = 1 + \zeta_+, \quad u_d = U_+, \quad \eta_u = 1 + \zeta_-, \quad u_u = U_-. \tag{3.4}$$

Using (3.4) and relationships (2.7), (2.9), (2.10), (2.11) we obtain the system for $\eta_{u,d}$, $u_{u,d}$,

$$\eta_u u_u = \eta_d u_d, \quad \tfrac{1}{2}(u_u)^2 + \eta_u = \tfrac{1}{2}(u_d)^2 + \eta_d, \quad \tfrac{1}{2}(u_u)^2 + \eta_u - \tfrac{3}{2}(\eta_u u_u)^{2/3} = f_m, \tag{3.5}$$

which is closed by any of two (asymptotically equivalent) conditions:

$$u_u + 2\sqrt{\eta_u} = F + 2 \tag{3.6}$$

or

$$u_d + 2\sqrt{\eta_d} = F + 2. \tag{3.7}$$

Both the hydraulic elevation (3.2) upstream and the depression (3.3) downstream are resolved into the undisturbed flow $\eta = 1, u = F$ by expanding undular bores. These undular bores represent nonlinear modulated periodic wavetrains and can be described using the Whitham modulation theory (Whitham 1974).

Before we proceed with the undular bore analysis it is instructive to obtain simple approximate explicit expressions for $\eta_{u,d}$, $u_{u,d}$ in terms of F and f_m for weak topographies. We use the asymptotic closure conditions (3.6) , (3.7) to eliminate $\eta_{u,d}$ from (3.5) and obtain a single equation for $w = u_{u,d}$,

$$\frac{w^2}{2} + \left(\frac{F-w}{2} + 1\right)^2 - \frac{3}{2}\left[w\left(\frac{F-w}{2} + 1\right)^2\right]^{2/3} = f_m. \tag{3.8}$$

This equation has two roots, the larger one corresponds to u_d and the smaller one to u_u. It is easy to see that for $f_m = 0$ (3.8) is identically satisfied if $w = (F + 2)/3$. Expanding (3.8) for small f_m we obtain to first order

$$u_u = 1 + \frac{1}{3}(F-1) - \sqrt{\frac{2f_m}{3}}, \quad u_d = 1 + \frac{1}{3}(F-1) + \sqrt{\frac{2f_m}{3}}, \tag{3.9}$$

where we have also used that F takes its values in the transcritical region (see (2.4))

$$1 - \sqrt{\frac{3f_m}{2}} < F < 1 + \sqrt{\frac{3f_m}{2}}. \tag{3.10}$$

With the same accuracy we get, respectively, from (3.6), (3.7):

$$\eta_u = 1 + \frac{2}{3}(F-1) + \sqrt{\frac{2f_m}{3}}, \quad \eta_d = 1 + \frac{2}{3}(F-1) - \sqrt{\frac{2f_m}{3}}. \tag{3.11}$$

One can see that at the lower boundary, $F = F_-$, of the transcritical region one has $\eta_u = 1$, $\eta_d = 1 - 2(2f_m/3)^{1/2}$, that is, there is only the downstream jump. Similarly, if $F = F_+$, one has $\eta_d = 1$, $\eta_u = 1 + 2(2f_m/3)^{1/2}$, that is, there is only the upstream jump. As a matter of fact, this qualitative behaviour at the boundaries of the transcritical region is also characteristic for the resonant flows satisfying fully nonlinear conditions (3.5)–(3.7) (see figure 4).

Next we make a brief account of the properties of the travelling wave solutions to the SG system (1.1), (1.2) necessary for the asymptotic modulation description of

the SG undular bores. The periodic travelling wave solution of the SG system is expressed in terms of the Jacobian elliptic function $\mathrm{cn}(\theta;m)$ and depends on four constant parameters: c, $\eta_3 \geqslant \eta_2 \geqslant \eta_1 > 0$ (see El *et al.* 2006),

$$\eta(x,t) = \eta_2 + a\ \mathrm{cn}^2\left(\frac{1}{2}\sqrt{\frac{3(\eta_3-\eta_1)}{\eta_1\eta_2\eta_3}}(x-ct);m\right), \qquad u = c \mp \frac{(\eta_1\eta_2\eta_3)^{1/2}}{\eta}, \tag{3.12}$$

$$\text{where} \qquad a = \eta_3 - \eta_2, \qquad m = \frac{\eta_3-\eta_2}{\eta_3-\eta_1} \tag{3.13}$$

are the wave amplitude and the modulus respectively and c is the phase speed. Signs '$-$' and '$+$' in the expression (3.12) for the velocity u correspond to the right- and left-propagating waves respectively The wavenumber is given by

$$k = \sqrt{\frac{3(\eta_3-\eta_1)}{\eta_1\eta_2\eta_3}}\frac{\pi}{2K(m)}, \tag{3.14}$$

where $K(m)$ is the complete elliptic integral of the first kind. When $m \to 0$ (i.e. $\eta_2 \to \eta_3$) the cnoidal wave (3.12) transforms into the harmonic small-amplitude wave characterized by the dispersion relation

$$\omega_0(k;u_0,\eta_0) = ck = k\left(u_0 \pm \frac{\eta_0^{1/2}}{(1+\eta_0^2k^2/3)^{1/2}}\right), \tag{3.15}$$

where η_0, u_0 are the background flow parameters and the signs '$+$' and '$-$' correspond to the right- and left-propagating waves respectively. When $m = 1$ (i.e. $\eta_2 = \eta_1$) the wavenumber $k = 0$ and the cnoidal wave (3.12) becomes a solitary wave,

$$\eta = \eta_0 + a\ \mathrm{sech}^{-2}\left(\frac{\sqrt{3a}}{\eta_0\sqrt{\eta_0+a}}(x-c_st)\right) \tag{3.16}$$

characterized by the speed–amplitude relationship

$$c_s = u_0 \pm \sqrt{\eta_0+a}. \tag{3.17}$$

Here '$+$' corresponds to the right-propagating and '$-$' to the left-propagating solitary wave. In the undular bore solution, the local travelling wave parameters $\eta_1, \eta_2, \eta_3, c$ are allowed to slowly depend on x, t. As a result, their evolution is governed by the Whitham modulation equations, which can be obtained by averaging the conservation laws of the SG system over the period $2\pi/k$ of (3.12) or, alternatively, by the standard multiple-scale analysis (see Gavrilyuk 1994). As a matter of fact, one can use any four independent combinations of $\eta_1, \eta_2, \eta_3, c$ as modulation variables. The most convenient choice appears to be $\overline{\eta}, \overline{u}, k, \widetilde{k}$, where $\overline{\eta}$, $\overline{u}$ are the mean flow parameters defined as averages of η and u over the period of the travelling wave (3.12), k is the wavenumber (3.14), and

$$\widetilde{k} = \sqrt{\frac{3(\eta_3-\eta_1)}{\eta_1\eta_2\eta_3}}\frac{\pi}{2K(1-m)} \tag{3.18}$$

is the 'conjugate wavenumber' associated with the adjoint (imaginary) period of the elliptic solution (3.12) in the complex x plane. When $m = 1$, $\widetilde{k}$ becomes proportional to the inverse solitary wave half-width (sometimes called the soliton wavenumber). In the opposite limit, when $m = 0$, one also has $\widetilde{k} = 0$.

The modulations in the undular bore generated by the decay of an initial step in η and u are described by an appropriate similarity solution of the Whitham equations. To clarify how this applies to the present problem of the transcritical flow past topography we note that, since both downstream and upstream undular bores expand with time, for sufficiently large t one can neglect the topography width $2L$ compared with the width of the undular bore. Hence, on the typical scale of the modulation variations the hydraulic transition from (η_u, u_u) upstream to (η_d, u_d) downstream can be considered to be localized at $x=0$, which allows one to use similarity modulation solution for the description of the large-time behaviour of the flow. The required solution is chosen in such a way that it would provide continuous matching of the mean flow in the undular bore region with given external constant flow at free boundaries $x^- = s^- t$ and $x^+ = s^+ t$ defined by the conditions that $\tilde{k}=0$ at one (linear) edge and $k=0$ at the opposite (soliton) edge. In the left-propagating shallow-water undular bore the solitary wave forms at the leading edge $x^-(t)$ and the linear wave train degeneration occurs at the trailing edge $x^+(t)$. The crucial fact that enables one to determine the speeds $s^\pm$ of the undular bore edges in terms of the initial step parameters is that the boundaries of the undular bore, where the matching of the modulation solution with the external constant flow occurs, must necessarily be characteristics of the modulation Whitham system. Then the constraints imposed by the corresponding characteristic relationships along the linear group velocity $\mathrm{d}x/\mathrm{d}t = \partial\omega_0/\partial k$ and the soliton $\mathrm{d}x/\mathrm{d}t = (\omega/k)_{k=0}$ characteristics lead to two systems of ordinary differential equations for the undular bore edge parameters (see El 2005 for details). For the SG system these equations were derived and solved in El *et al.* (2006). However, the results of the latter paper cannot be directly applied to the present resonant flow problem as they should be first modified to the case of left-propagating waves and non-zero background velocity. The modification is quite straightforward and involves incorporation of the simple-wave relationship $\overline{u} + 2\overline{\eta}^{1/2} = F + 2$ for the background flow into the linear dispersion relation (3.15), namely we replace η_0, u_0 with $\overline{\eta}, \overline{u}$ so that one arrives at the dispersion relation for the *left-propagating* linear modulated waves riding on a slowly varying simple-wave hydrodynamic background

$$\Omega_0(\bar{\eta}, k) = \omega_0(k; \overline{u}(\overline{\eta}), \overline{\eta}) = k[F + 2(1 - \bar{\eta}^{1/2})] - \frac{k\bar{\eta}^{1/2}}{(1 + \bar{\eta}^2 k^2/3)^{1/2}}. \tag{3.19}$$

Then one constructs two families of characteristic integrals I_1, I_2 of the modulation system specified by the ordinary differential equations (see El *et al.* 2006, 2008 for details):

$$I_1: \qquad \widetilde{k} = 0, \quad \frac{\mathrm{d}k}{\mathrm{d}\overline{\eta}} = \frac{\partial\Omega_0/\partial\overline{\eta}}{V(\overline{\eta}) - \partial\Omega_0/\partial k} \quad \text{on} \quad \frac{\mathrm{d}x}{\mathrm{d}t} = \frac{\partial\Omega_0}{\partial k}, \tag{3.20}$$

$$I_2: \qquad k = 0, \quad \frac{\mathrm{d}\widetilde{k}}{\mathrm{d}\overline{\eta}} = \frac{\partial\widetilde{\Omega}_0/\partial\overline{\eta}}{V(\overline{\eta}) - \partial\widetilde{\Omega}_0/\partial\widetilde{k}} \quad \text{on} \quad \frac{\mathrm{d}x}{\mathrm{d}t} = \frac{\widetilde{\Omega}_0}{\widetilde{k}}. \tag{3.21}$$

Here

$$V(\overline{\eta}) = \overline{u}(\overline{\eta}) - \overline{\eta}^{1/2} = F + 2 - 3\overline{\eta}^{1/2} \tag{3.22}$$

is the characteristic velocity of the left-propagating simple wave of the ideal shallow-water equations (i.e. the dispersionless limit of the SG system) and

$$\widetilde{\Omega}_0(\overline{\eta}, \widetilde{k}) = -\mathrm{i}\Omega_0(\overline{\eta}, \mathrm{i}\widetilde{k}) = \widetilde{k}(F + 2(1 - \overline{\eta}^{1/2})) + \frac{\widetilde{k}\overline{\eta}^{1/2}}{(1 - \overline{\eta}^2\widetilde{k}^2/3)^{1/2}} \tag{3.23}$$

is the SG 'solitary wave dispersion relation'. Ordinary differential equations (3.20) and (3.21) for $k(\overline{\eta})$ and $\widetilde{k}(\overline{\eta})$ are readily integrated using the substitutions $\alpha=(1+k^2\overline{\eta}^2/3)^{-1/2}$ and $\widetilde{\alpha}=(1-\widetilde{k}^2\overline{\eta}^2/3)^{-1/2}$ respectively,

$$\frac{\overline{\eta}}{\lambda_1}=\frac{1}{\alpha^{1/2}}\left(\frac{4-\alpha}{3}\right)^{21/10}\left(\frac{1+\alpha}{2}\right)^{2/5}, \tag{3.24}$$

$$\frac{\overline{\eta}}{\lambda_2}=\frac{1}{\widetilde{\alpha}^{1/2}}\left(\frac{4-\widetilde{\alpha}}{3}\right)^{21/10}\left(\frac{1+\widetilde{\alpha}}{2}\right)^{2/5}. \tag{3.25}$$

Here $\lambda_{1,2}$ are constants of integration, their values are to be found from the free-boundary matching conditions for downstream and upstream undular bores separately.

3.3. *Downstream undular bore*

We first assume that the downstream undular bore is fully realized (as in figure 6*a*) so that it connects the undisturbed flow $\eta=1, u=F$ at the trailing edge x_d^+ with the hydraulic transition downstream state $\eta=\eta_d,\ u=u_d$ at the leading edge x_d^- (we use the terms 'trailing' and 'leading' here keeping in mind that we deal with the waves based on the left-propagating family of characteristics, so that the leading edge is, as usual, associated with the solitary wave) and satisfies the transition condition (3.7). Then the matching conditions at the edges $x_d^\pm=s_d^\pm t$ are

$$\text{at}\quad x=s_d^-\,t:\qquad k=0,\quad \bar{\eta}=\eta_d,\quad \bar{u}=u_d, \tag{3.26}$$

$$\text{at}\quad x=s_d^+\,t:\qquad \widetilde{k}=0,\quad \bar{\eta}=1,\quad \bar{u}=F. \tag{3.27}$$

So the downstream undular bore transition is located in the interval $s_d^-\,t<x<s_d^+\,t$ and is characterized by two independent parameters: η_d and F. Our task is to determine the dependence of the edge speeds $s_d^\pm$ and the amplitude of the leading solitary wave a_d^- on these two parameters. First we apply the matching conditions (3.26) and (3.27) to the solutions (3.24), (3.25) respectively to obtain $\lambda_1=\eta_d$, $\lambda_2=1$ (see El *et al.* 2006, 2008 for a detailed explanation). Thus, the characteristic integrals $k(\overline{\eta})$ and $\widetilde{k}(\overline{\eta})$ for the downstream flow are now completely determined by (3.24) and (3.25).

The speeds of the undular bore edges are defined by the kinematic conditions which state that the speeds of the edges should be equal to the respective characteristic (group) velocities of the nonlinear wave train at its endpoints where $m=0$ and $m=1$ (see El 2005). The trailing (harmonic, $m=0$) edge x_d^+ rides on the background $\eta=1$ with the linear group velocity

$$s_d^+=\frac{\partial\Omega_0}{\partial k}|_{\overline{\eta}=1,\ k=k^+}, \tag{3.28}$$

where $k^+=k(\overline{\eta}=1)$ is found from (3.24). Now using (3.19) we get an implicit expression for the trailing edge speed s_d^+ in terms of η_d and the Froude number F of the undisturbed flow

$$\frac{\sqrt{\beta}}{\eta_d}-\left(\frac{4-\beta}{3}\right)^{21/10}\left(\frac{1+\beta}{2}\right)^{2/5}=0,\quad \text{where}\quad \beta=(F-s_d^+)^{1/3}. \tag{3.29}$$

One should note that the notion of the trailing edge of an undular bore is rather theoretical since the trailing edge, as it is defined by the modulation theory, is associated with the group of small-amplitude waves rather than with a particular

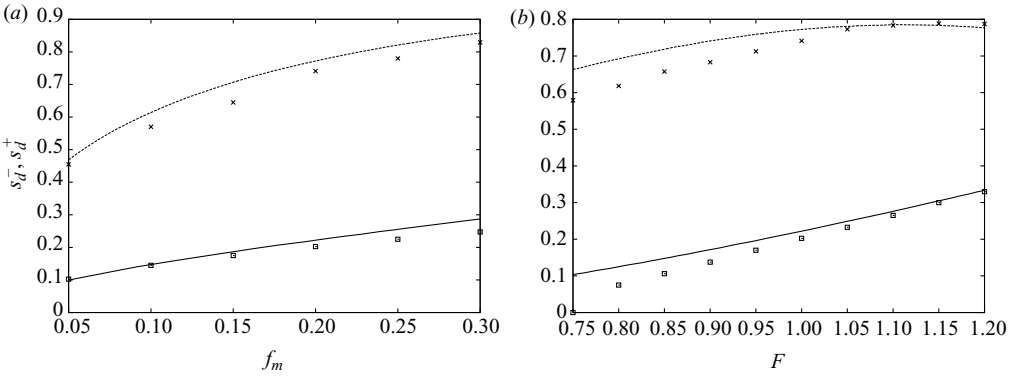

FIGURE 8. Dependence of the downstream undular bore edge speeds $s_d^{\pm}$ on the forcing amplitude f_m for the fixed Froude number $F=1$ (a) and on the Froude number F for the fixed forcing amplitude $f_m=0.2$ (b). Lines: modulation solutions for s_d^- (solid) and s_d^+ (broken); symbols: the values of $s_d^{\pm}$ extracted from the numerical solutions.

wave crest so, unlike the leading edge specified by a soliton, the trailing edge is often not clearly pronounced in numerical simulations (and in physical observations). However, this notion is very useful as it enables one to define the undular bore width and, in particular, to quantify the differences between different models with respect to the rate of the 'wave production' (see for instance Lamb & Yan 1996 for the relevant numerical comparisons for undular bores modelled by different KdV type models and full Euler equations, and El *et al.* 2006 for the comparison between the KdV and SG undular bores).

The leading (soliton, $m=1$) edge x_d^- propagates on the background $\eta=\eta_d$ with the soliton velocity

$$s_d^- = \frac{\widetilde{\Omega}_0(\eta_d, \widetilde{k}^-)}{\widetilde{k}^-}, \tag{3.30}$$

where $\widetilde{k}^- = \widetilde{k}(\overline{\eta}=\eta_d)$ is found from (3.25) (see El 2005 for the derivation of (3.30)). Now, using expression (3.23) for the conjugate frequency we obtain from (3.30) an implicit equation for the leading edge speed $s_d^- = s_d^-(\eta_d, F)$,

$$\eta_d\sqrt{\gamma} - \left(\frac{4-\gamma}{3}\right)^{21/10}\left(\frac{1+\gamma}{2}\right)^{2/5} = 0, \quad \text{where} \quad \gamma = (2+F-s_d^-)\eta_d^{-1/2} - 2. \tag{3.31}$$

Next, having the dependence η_d on f_m and F from (3.5), (3.7) we finally get the downstream undular bore edge speeds $s_d^{\pm}$ as functions of the input parameters f_m, F. The dependencies of $s_d^{\pm}$ on f_m (for the fixed value $F=1$) and on F (for the fixed value $f_m=0.2$) are shown in figure 8. The symbols in the same figure show the values of $s_d^{\pm}$ extracted from the numerical solutions of the forced SG system (in numerics the point of the trailing edge was determined using simple linear approximation in x of the undular bore envelope, which agrees with the asymptotic behaviour of the SG modulation solution near the trailing edge – see El *et al.* 2006). One can see that the modulation theory predicts the location of the undular bores very well. The growing discrepancy between numerical and modulation solutions as one gets closer the lower transcritical boundary, which is $F=F_-\approx 0.55$ for $f_m=0.2$, seen in the dependence on the Froude number, is explained by the fact that $F=F_-$ is the point of the downstream bifurcation and the local hydraulic approximation does not work very

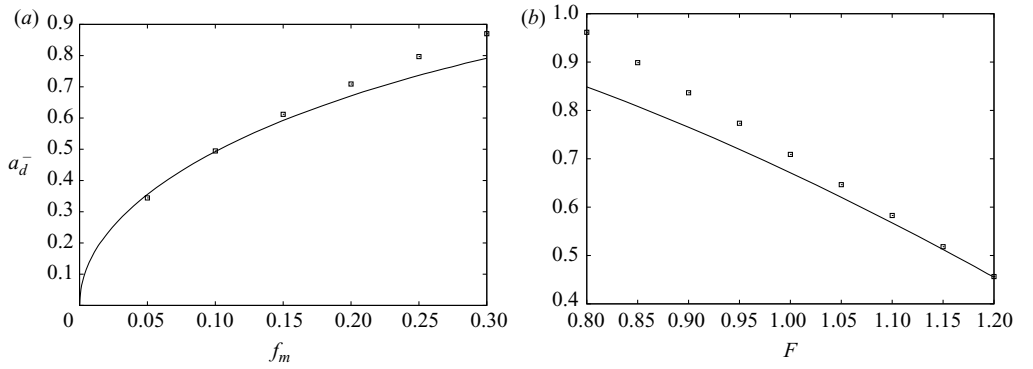

FIGURE 9. Dependence of the downstream undular bore leading soliton amplitude a_d^- on the forcing amplitude f_m for the fixed Froude number $F=1$ (a) and on the Froude number F for the fixed forcing amplitude $f_m=0.2$ (b). Solid line: modulation solution (3.32) for a^-; symbols: values of a^- extracted from the numerical solutions.

well downstream for the flows with the Froude numbers close to this value (see the discussion in the end of § 2.2).

Since the leading edge is defined by a solitary wave, we have $s_d^- = c_s(\eta_d, u_d, a_d^-)$ where $c_s(\eta, u, a)$ is the SG soliton speed–amplitude relation (3.17) and η_d and u_d are related through the transition condition (3.7), we have for the lead soliton amplitude a_d^-:

$$a_d^- = (F - s_d^- + 2(1 - \sqrt{\eta_d}))^2 - \eta_d. \tag{3.32}$$

Dependencies of the soliton amplitude a_d^- on f_m and F given by (3.32), (3.31), (3.5), (3.7) is presented in figure 9. Again, one cam see a very good agreement between analytical and numerical dependencies on f_m and noticeable discrepancy between the dependencies on the Froude number as the lower transcritical boundary is approached. This departure of the actual behaviour of the flow from the prediction of the analytical solution constructed under the assumption of the existence of a local steady hydraulic transition is to be expected (see the discussion at the end of § 2). Still, within the range of applicability of the SG system to the description of finite-amplitude laminar shallow-water flow, which, for the chosen value $f_m=0.2$, involves the Froude numbers from about $F\approx 1.0$ to $F=F_+\approx 1.55$ (and soliton amplitudes from $a=0$ to $a\approx 0.6$) the agreement is quite good.

For weak topographies we use expansion (3.11) for η_d to obtain approximate explicit expressions for $s_d^{\pm}$ and a_d^- in terms of f_m and F. Clearly if $f_m=0$ we have $\eta_d=1$, $F=1$, $s_d^{\pm}=0$. Then from (3.29), (3.31), (3.32) we obtain to first order in $(F-1)$ and $(f_m)^{1/2}$

$$s_d^- = \frac{2}{3}(F-1) + \frac{1}{2}\sqrt{\frac{2f_m}{3}}, \quad s_d^+ = -(F-1) + 3\sqrt{\frac{2f_m}{3}}, \tag{3.33}$$

$$a_d^- = -\frac{4}{3}(F-1) + 2\sqrt{\frac{2f_m}{3}} \tag{3.34}$$

provided $F_- < F < F_+$ (see (3.10)). Expansions (3.33) and (3.34) correspond to the forced KdV approximation (Grimshaw & Smyth 1986 and Smyth 1987) (note that the coefficients in (3.33) correspond to the KdV equation in the form 'naturally' following from the small-amplitude long-wave expansions of the SG equations, see Johnson 2002 or El *et al.* 2006, without its further reduction to the standard form

as in Grimshaw & Smyth 1986 and Smyth 1987). Equation (3.34) reproduces the classical result of Gurevich & Pitaevskii (1974) $a_{max} = 2\delta$ where a_{max} is the amplitude of the greatest soliton in the undular bore and δ is the initial step value (in our case the downstream step is $\delta = 1 - \eta_d$); this result does not depend on the normalization of the KdV equation.

One can see from (3.33) that for the transcritical interval of F (3.10) the value s_d^- can change its sign, which implies that for certain domain of values of F and f_m the downstream undular bore would propagate upstream. Since this is not allowed, the bore should be terminated at $x = 0$ so that it gets realized only partially for $0 < x < s_d^+ t$, with the modulus m ranging within the interval $0 \leqslant m \leqslant m^*$, where $m^* < 1$ is certain cutoff value. The line in the f_m, F plane defining the parameter values at which the downstream bore gets attached to to the topography at its leading edge is specified by the equation $s_d^- = 0$, s_d^- being defined by (3.31). This line is shown in figure 5 where it separates regions II and III. A more detailed discussion of partial undular bores will be given in the next subsection.

3.4. *Upstream undular bore*

The upstream undular bore connects the undisturbed flow $\eta = 1$, $u = F$ at the leading edge with the hydraulic transition upstream state $\eta = \eta_u$, $u = u_u$ at the trailing edge and satisfies the transition condition (3.6). Again, we first assume that the upstream undular bore is fully realized. Then the matching conditions at the leading $x_u^- = s_u^- t$ and trailing $x_u^+ = s_u^+ t$ edges are

$$\text{at} \quad x = s_u^- t: \qquad k = 0, \quad \bar{\eta} = 1, \quad \bar{u} = F, \tag{3.35}$$

$$\text{at} \quad x = s_u^+ t: \qquad \widetilde{k} = 0, \quad \bar{\eta} = \eta_u, \quad \bar{u} = u_u. \tag{3.36}$$

The upstream undular bore occupies an expanding zone $s_u^- t < x < s_u^+ t$ and is characterized by two independent parameters: η_u and F. Similar to the downstream case, our task is to determine dependence of the edge speeds $s_u^\pm$ on these two parameters. As before, we apply the matching conditions (3.35) and (3.36) to the solutions (3.24), (3.25) respectively to obtain now $\lambda_1 = 1$, $\lambda_2 = \eta_u$. The characteristic integrals $k(\bar{\eta})$ and $\widetilde{k}(\bar{\eta})$ for the upstream flow are now completely determined by (3.24) and (3.25).

The kinematic conditions defining the speeds of the edges of the upstream undular bore have the form (cf. (3.28), (3.30))

$$s_u^+ = \frac{\partial \Omega_0}{\partial k}|_{\eta = \eta_u, \ k = k^+}, \qquad s_u^- = \frac{\widetilde{\Omega}_0(1, \tilde{k}^-)}{\tilde{k}^-}. \tag{3.37}$$

The parameters k^+ and $\tilde{k}^-$ in (3.37) are calculated as the boundary values $k^+ = k(\eta_u)$, $\tilde{k}^- = \tilde{k}(1)$ of the functions $k(\bar{\eta})$ and $\tilde{k}(\bar{\eta})$.

Next, using (3.37), (3.19) we get an implicit expression for the trailing (harmonic) edge s_u^+ in terms of η_u:

$$\sqrt{\beta}\eta_u - \left(\frac{4-\beta}{3}\right)^{21/10}\left(\frac{1+\beta}{2}\right)^{2/5} = 0, \quad \text{where} \quad \beta = \left(\frac{2 + F - s_u^+}{\sqrt{\eta_u}} - 2\right)^{1/3}. \tag{3.38}$$

Similarly, using the expression for the conjugate frequency (3.23) we obtain from (3.37) the equation of the leading (soliton) edge $s_u^-(\eta_u, F)$ in an implicit form,

$$\frac{\sqrt{\gamma}}{\eta_u} - \left(\frac{4-\gamma}{3}\right)^{21/10}\left(\frac{1+\gamma}{2}\right)^{2/5} = 0, \quad \text{where} \quad \gamma = F - s_u^-. \tag{3.39}$$

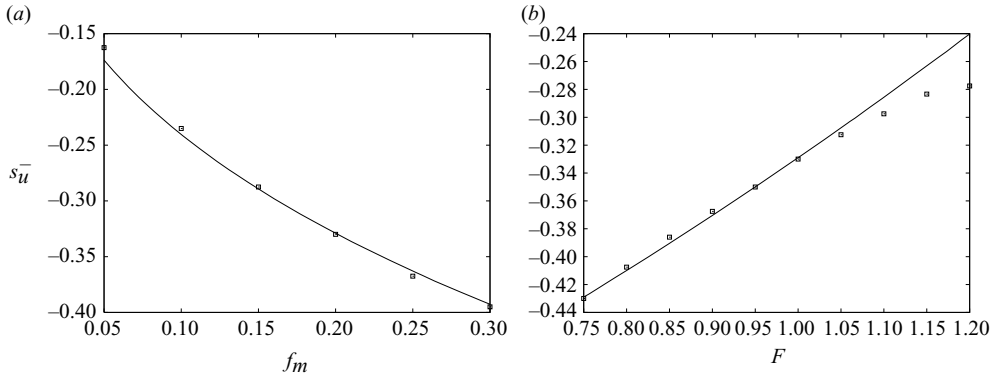

FIGURE 10. Dependence of the upstream lead soliton speed s_u^- on the forcing amplitude f_m for the fixed Froude number $F=1$ (a) and on the Froude number F for the fixed forcing amplitude $f_m=0.2$ (b). Line: modulation solutions for s_u^-; symbols: the values of s_u^- extracted from the numerical solutions.

Now, having the dependence η_u on f_m, F specified by (3.5), (3.6) we get the speeds $s_u^{\pm}$ as functions of the input parameters f_m, F. The dependencies of $s_u^{\pm}$ on F (for the fixed value $f_m=0.2$) and on f_m (for the fixed value $F=1$) are shown in figure 10.

One can see from the leading edge curve in figure 10 that for certain interval of Froude number values we have $s_u^+>0$ which implies that the upstream undular bore partially propagates downstream. This can already be seen from the small amplitude, $f_m \ll 1$, expansions of (3.38), (3.39) analogous to (3.33)

$$s_u^- = \frac{1}{3}(F-1) - \sqrt{\frac{2f_m}{3}}, \qquad s_u^+ = 2(F-1) + \frac{3}{2}\sqrt{\frac{2f_m}{3}}. \tag{3.40}$$

Indeed, one can readily see that for F in the transcritical interval (3.10) one has $s_u^+>0$. Obviously, this is not allowed as the upstream modulation wavetrain is only defined for $x<0$ so the modulation solution must be terminated at $x=0$ resulting in a partial undular bore, which can be viewed as a soliton train propagating upstream. The formal grounds for the possibility of 'cutting' the undular bore in two can be inferred from the detailed modulation analysis available in the case of weak topography forcing described by the forced KdV equation and studied in El *et al.* (2006) and Smyth (1987). The idea is that, since the modulation solution represents a centred characteristic fan of the Whitham equations (Whitham 1974), and for the edge characteristics we have $\mathrm{d}x/\mathrm{d}t=s^-<0$ and $\mathrm{d}x/\mathrm{d}t=s^+>0$, there should be a characteristic $\mathrm{d}x/\mathrm{d}t=0$ for the solution under study. Then the free-boundary matching condition at the unknown boundary $x^+>0$ (condition (3.36) in the present SG case) can be replaced by the appropriate boundary conditions at $x=0$ leading to the same modulation solution for $x<0$. The boundary conditions should be formulated in terms of the *Riemann invariants* of the modulation system as the Riemann invariants are transferred to the boundary $x=0$ along the corresponding modulation characteristics from the given initial step data. As a result, to construct the modulation solution for the upstream partial undular bore generated by a given hydraulic jump at $x=0$ one just considers the part of the modulation solution in the region $x<0$ *as if* the undular bore was created by the decay of the initial step located at $x=0$ and having the same magnitude as the boundary jump. This is essentially how the modulation solution for the upstream partial undular bore was constructed in Grimshaw & Smyth (1986) and Smyth (1987).

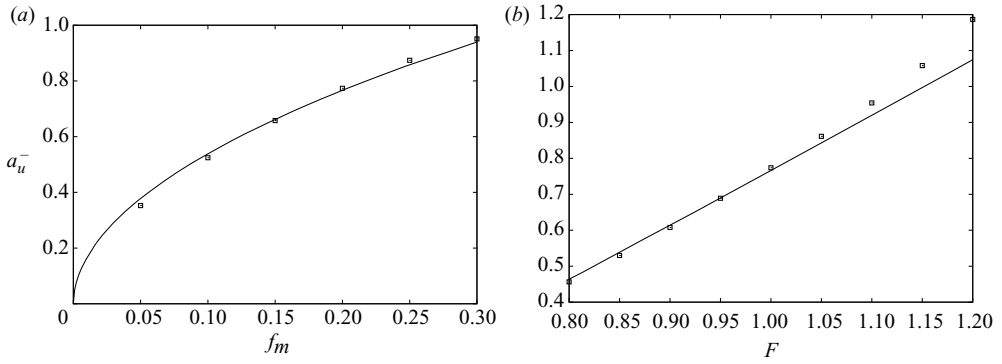

FIGURE 11. Dependence of the upstream lead soliton amplitude a_u^- on the forcing amplitude f_m for the fixed Froude number $F=1$ (a) and on the Froude number F for the fixed forcing amplitude $f_m=0.2$ (b). Line: modulation solutions for a_u^-; symbols: the values of a_u^- extracted from the numerical solutions.

Although the Riemann invariants are not available for the modulation system associated with the SG equations, one can argue that the values of the 'external' hydrodynamic invariants $\lambda_\pm = u/2 \pm \sqrt{\eta}$ are transferred across the modulation zone with the same effect on the edge speeds $s^\pm$ as if they were present within the undular bore (see Tyurina & El 1999; El 2005; El *et al.* 2005); so one can use the value of s_u^- (3.39) to characterize the upstream partial undular bore of the SG system. For the tallest upstream soliton we have $s_u^- = c_s(1, F, a_u^-)$ where $c_s(\overline{\eta}, \overline{u}, a)$ is the speed–amplitude relation (3.17). Thus for the soliton amplitude a_u^- we have

$$a_u^- = (F - s_u^-)^2 - 1. \tag{3.41}$$

Using (3.5), (3.7), (3.39), (3.41) one obtains the dependence of the upstream lead soliton amplitude a_u^- on f_m and F. The dependencies of s_u^- and a_u^- on the topography height f_m and the Froude number of the equilibrium flow are presented in figures 10 and 11. One can see an excellent agreement between the analytical and numerical dependencies on f_m. The discrepancy between the theory and numerics seen in the comparisons for the Froude number dependencies as one gets closer to the upper transcritical boundary $F = F_+$ is connected with the already discussed unsteady character of the flow over the forcing range for the flows with Froude numbers near the upstream bifurcation point $F = F_+$.

For weakly nonlinear case, $f_m \ll 1$, we have

$$a_u^- = \frac{4}{3}(F-1) + 2\sqrt{\frac{2f_m}{3}}, \tag{3.42}$$

which again agrees with the classical KdV result $a_{max} = 2\delta$ where $\delta = \eta_u - 1$ is the value of the equivalent initial step (see (3.11) for the weak forcing expansion of η_u).

3.5. *Drag force*

The drag force on the topography is (see for instance Baines 1995)

$$F_D = \int_{-L}^{L} p_{z=d}\, d_x \, \mathrm{d}x, \tag{3.43}$$

where $p_{z=d}$ is the pressure evaluated at the bottom $z = d = 1 - f$. Here, in the SG system, to leading order the pressure field is just $p = \zeta$ (see the Appendix), and so we

can write

$$F_D = -\int_{-L}^{L} H f_x \, \mathrm{d}x, \tag{3.44}$$

where we recall that $H = 1 + \zeta - f$. Further, since we are assuming that the flow is locally steady over the topography, we can use the expressions (2.1) to evaluate F_D giving (see Baines 1995)

$$F_D = \frac{(\eta_d - \eta_u)^3}{2\eta_d \eta_u}, \tag{3.45}$$

where, we recall, $\eta_d = H(-L)$, $\eta_u = H(L)$. For the case when both undular bores are completely detached from the topography (the region III in figure 5) expression (3.45) together with formulae (3.5)–(3.7) determines the stationary value of the drag force. In this case for weak topographies we obtain using the expansions (3.11),

$$F_D = -32\left(\frac{f_m}{6}\right)^{3/2}\left(1 - \frac{4}{3}(F-1)\right) + \cdots. \tag{3.46}$$

However, when one of the undular bores gets attached to the topography, the corresponding value η_u or η_d at the attachment point will oscillate resulting in oscillations of the drag force with the same frequency. Below we derive an approximate formula for the drag force frequency for the most typical upstream attachment case assuming that the partial undular bore can be viewed as a soliton train (see figure 6*a*). For the forced KdV equation such a soliton train approximation proved to work very well (see Grimshaw & Smyth 1986 and Smyth 1987).

The frequency of the upstream undular bore at the point of attachment (hence the drag force frequency) is calculated by the formula

$$\omega_D = -k^* c^*, \tag{3.47}$$

where k^* and $c^* < 0$ are respectively the upstream wavenumber and phase velocity at $x = 0$. Assuming that the upstream undular bore can be viewed as a soliton train with the solitons having almost the same amplitude, we take $c^* = s_u^-$.

To estimate k^* we make use of the fact that wavenumber function $k(x, t)$ is almost linear in x through the entire undular bore except for the vicinity of the leading edge, where k rather rapidly decays to zero ($\mathrm{d}k/\mathrm{d}x \to \infty$ as x approaches the leading edge – see, for instance, the full modulation solution for the KdV undular bore in Gurevich & Pitaevskii 1974 or Fornberg & Whitham 1978). The linear approximation for $k(x, t)$ near the trailing edge for the simple SG undular was obtained in El *et al.* (2006) (see formula (65) in the referred paper).

For our case of the left-propagating bore this approximation assumes the form

$$k \approx k^+ - \frac{2}{3\omega_0''(k^+)}\left(s_u^+ - \frac{x}{t}\right), \tag{3.48}$$

where

$$\omega_0''(k) = \frac{k \cdot \eta_u^{5/2}}{(1 + k^2\eta_u^2/3)^{5/2}} \tag{3.49}$$

is the second derivative of the SG dispersion relation (3.15) for the linear waves propagating to the left against the background $\eta = \eta_u$; k^+ being the value of the wavenumber at the trailing edge of the upstream undular bore and s_u^+ the speed of its trailing edge. We note that the trailing edge of the upstream undular bore is not physically realized in the flow, as the upstream bore is terminated at $x = 0$.

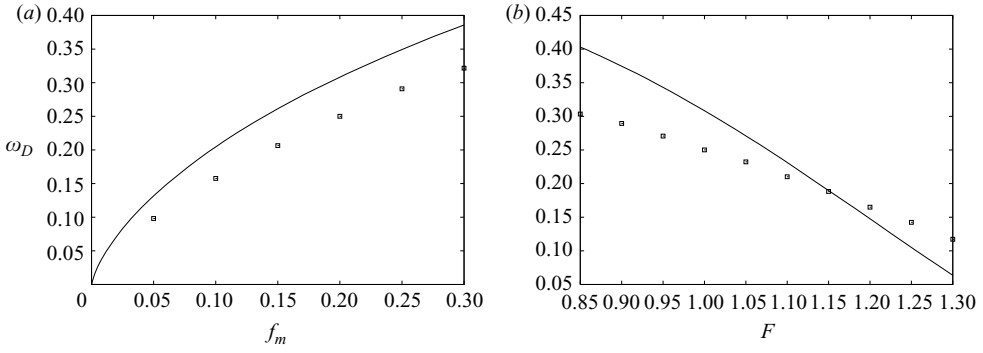

FIGURE 12. Dependence of the drag force frequency ω_D on the forcing amplitude f_m for the fixed Froude number $F=1$ (a) and on the Froude number F for the fixed forcing amplitude $f_m=0.2$ (b). Line: approximate formula (3.52); symbols: the values of ω_D extracted from the numerical solutions.

However, as was explained in §4.4, all the parameters of the upstream undular bore are consistent with the definition (3.37) of the trailing edge *as if* it existed. So we find the 'effective' trailing edge wavenumber k^+ from (3.37), i.e. from

$$s_u^+ = \frac{\partial \Omega_0}{\partial k}|_{\eta=\eta_u,\ k=k^+} = F + 2\left(1-\eta_u^{1/2}\right) - \frac{\eta_u^{1/2}}{(1+(k^+)^2(\eta_u)^2/3)^{3/2}}. \tag{3.50}$$

Since s_u^+ is given by formula (3.38) the quantity k^+ is now completely defined and we obtain at the point of attachment

$$k^* = k(x=0) \approx k^+ - \frac{2s_u^+}{3\omega_0''(k^+)}. \tag{3.51}$$

Now substituting k^*, c^* into (3.47) we obtain an approximate formula for the frequency of the drag force oscillations

$$\omega_D \approx s_u^- \left(\frac{2}{3}\frac{s_u^+}{\omega_0''(k^+)} - k^+\right). \tag{3.52}$$

We note that, while formula (3.52) represents a rather crude approximation, it can still be useful for the determination of approximate values for and general tendencies in the behaviour of the drag force frequency. Comparisons of the approximate behaviour given by (3.52) with the dependencies of the drag force frequency on f_m (for fixed $F=1$) and on F (for fixed $f_m=2$) obtained from our numerical simulations are shown in figure 12. One can see that, whilst the accuracy of the formula (3.52) is not particularly great, it correctly reproduces the approximate range and main features of the actual drag frequency behaviour.

4. Discussion

In this paper we have used the forced SG equations (1.1), (1.2) to describe transcritical irrotational flow over a localized obstacle, with the aim of extending the well-known fKdV model to finite-amplitude water waves.

As for the fKdV equation, the asymptotic solution consists of two parts, a steady hydraulic solution over the obstacle with upstream and downstream hydraulic jumps,

and the resolution of these jumps by undular bores using the Whitham modulation theory. In contrast to the fKdV model, the local hydraulic solution is fully nonlinear, but a full asymptotic description of the undular bores is not available, and instead we evaluate key parameters such as the amplitude of the leading wave and the location of the bores. The theoretical results are favourably compared with numerical simulations of the full forced SG system.

We would like to stress several qualitatively new results from our analysis. First, by using the undular bore closure of El *et al.* (2006) and expanding the transcritical hydraulic solution up to third order in amplitude we have shown that this solution implies an approximate (up to third order) conservation, across the topographic forcing region, of one of the Riemann invariants corresponding to the simple wave of the ideal dispersionless shallow water equations. The direction of propagation of this simple wave is opposite to that of the oncoming flow. This asymptotic conservation property eliminates the need for the introduction of an additional rarefraction wave downstream, which could theoretically be present in the downstream solution. Some evidence for such a very small rarefraction wave can be seen in the numerical simulations. The approximate conservation of the shallow water Riemann invariant across the topographic forcing also formally justifies the applicability of the unidirectional fKdV equation for the modelling of transcritical flows over weak topography. The second qualitatively new feature is the existence, in the plane of parameter values of the topographic forcing amplitude f_m and Froude number F of the oncoming flow, of a region corresponding to the generation of two fully detached undular bores (region III in figure 5). This is different from the prediction of the fKDV theory (see Grimshaw & Smyth 1986 and Smyth 1987) for which one of the bores is always attached to the forcing. Our preliminary comparisons with the corresponding solutions of the full Euler equations show that the these new features of the forced SG model are indeed present in the full Euler dynamics. A detailed comparison of the transcritical SG solutions with the corresponding solutions of the full Euler system is beyond the scope of this paper and will be presented elsewhere.

We also note that in practice, and certainly in the context of the fully nonlinear Euler equations, sufficiently large amplitude waves will break, whereas breaking does not occur in the present SG system. However, a typical wave breaking criterion might be $\zeta > 0.88$ (see Mei 1983 for instance), and we have ensured that in our present simulations we used forcing amplitudes and Froude numbers which produced waves below this threshold amplitude.

The corresponding range of the forcing amplitude f_m and of the oncoming Froude number F can be estimated by substituting this critical value of the amplitude into expressions (3.32) and (3.41) for the leading solitary wave amplitudes in the downstream and upstream waves respectively. Say, for $F = 1$ this gives the maximum admissible value of f_m of about 0.3 (see figures 9 and 11). Similarly, for a given $f_m = 0.2$ we obtain that the requirement that both undular bores are laminar implies that the admissible range for the oncoming flow Froude number is from about 0.9 to about 1.1. Of course, if one is interested in the non-breaking condition only for one of the bores, the admissible range of Froude numbers broadens.

Overall, for the moderate forcing amplitudes considered here, our results confirm that most features of the fKdV description hold up qualitatively for finite amplitude waves, while the quantitative description can be obtained in the framework of the forced SG system.

We would like to acknowledge the useful discussions with A. M. Kamchatnov.

Appendix. Derivation of forced SG equations

This derivation follows Camassa, Holm & Levermore (1997). The full Euler equations for two-dimensional irrotational flow of an inviscid fluid over topography are

$$u_t + uu_x + wu_z + p_x = 0, \tag{A 1}$$

$$w_t + uw_x + ww_z + p_z = 0, \tag{A 2}$$

$$u_x + w_z = 0, \tag{A 3}$$

valid in the region $-d < z < \zeta (d = 1 - f)$, where p is the dynamic pressure per unit density, defined so that the full pressure is $p + z$. These equations are expressed in non-dimensional units, based on a length scale h, the undisturbed fluid depth at infinity, a velocity scale $\sqrt{gh}$ and a time scale $\sqrt{h/g}$. The boundary conditions are that

$$w + ud_x = 0 \quad \text{at} \quad z = -d, \tag{A 4}$$

$$w - \zeta_t - u\zeta_x = 0 \quad \text{at} \quad z = \zeta, \tag{A 5}$$

$$p - \zeta = 0 \quad \text{at} \quad z = \zeta. \tag{A 6}$$

The equation for conservation of mass then follows, namely

$$\zeta_t + (HU)_x = 0, \tag{A 7}$$

$$\text{where} \quad H = d + \zeta, \quad HU = \int_{-d}^{\zeta} u \, \mathrm{d}z. \tag{A 8}$$

This is just (1.1). The horizontal momentum equation (A 1) can also be integrated over the depth to yield

$$(HU)_t + \left(\int_{-d}^{\zeta} u^2 \, dz \right)_x + \int_{-d}^{\zeta} p_x \, \mathrm{d}z = 0, \tag{A 9}$$

This will yield the second equation (1.2) after the integral terms have been approximately evaluated.

To evaluate the integral terms we make a long-wave expansion, in which $\partial/\partial x \sim \epsilon \ll 1$, and expand in powers of ϵ. First, we note that the flow is irrotational, that is,

$$u_z = w_x, \quad \text{in} \quad -d < z < \zeta. \tag{A 10}$$

Combining this with the incompressibility condition (A 3), we see that u, w each satisfy Laplace's equation. Then taking account of the boundary condition (A 4) we find that to the second order in ϵ,

$$u = \tilde{U}(x,t) - (2\tilde{U}_x d_x + \tilde{U} d_{xx})(z + d) - \frac{1}{2}\tilde{U}_{xx}(z + d)^2 + \cdots, \tag{A 11}$$

$$w = -d_x \tilde{U} - \tilde{U}_x (z + d) + \cdots. \tag{A 12}$$

Next we substitute (A 11) into (A 8) to get

$$U = \tilde{U} - (2\tilde{U}_x d_x + \tilde{U} d_{xx})\frac{H}{2} - \frac{H^2}{6}\tilde{U}_{xx} + \cdots, \tag{A 13}$$

$$\text{or} \quad \tilde{U} = U + (2U_x d_x + U d_{xx})\frac{H}{2} + \frac{H^2}{6}U_{xx} + \cdots. \tag{A 14}$$

The expression (A 11) is then substituted into the second term in (A 9) to yield

$$\int_{-d}^{\zeta} u^2 \,\mathrm{d}z = HU^2 + \cdots . \tag{A 15}$$

Finally, the pressure gradient is evaluated from (A 2) to yield

$$p_z = p_1(z+d)+p_2, \quad \text{where} \quad p_1 = DU_x - U_x^2, \;\; p_2 = D(d_x U), \quad D = \frac{\partial}{\partial t} + U\frac{\partial}{\partial x}. \tag{A 16}$$

With the boundary condition (A 6) this can then be integrated to yield the pressure and hence

$$\int_{-d}^{\zeta} p_x \,\mathrm{d}z = H\zeta_x - \frac{(H^3 p_1)_x}{3} - \frac{(H^2 p_2)_x}{2} + \frac{H^2 p_1 d_x}{2} + H p_2 d_x, \tag{A 17}$$

Finally, using the conservation of mass equation (A 7) this can be rewritten as

$$\int_{-d}^{\zeta} p_x \,\mathrm{d}z = H\zeta_x + \frac{(H^2 D^2 H)_x}{3} - \frac{(H^2 D^2 d)_x}{2} - \frac{H d_x}{2} D^2(\zeta - d). \tag{A 18}$$

Setting $d = 1 - f$ we recover (1.2).

REFERENCES

Baines, P. G. 1995 *Topographic Effects in Stratified Flows*. Cambridge University Press.

Camassa, R., Holm, D. D. & Levermore, C. D. 1997 Long-time shallow-water equations with a varying bottom. *J. Fluid Mech.* **349**, 173–189.

Dellar, P. J. 2003 Dispersive shallow water magnetohydrodynamics. *Phys. Plasmas* **10**, 581–590.

El, G. A. 2005 Resolution of a shock in hyperbolic systems modified by weak dispersion. *Chaos* **15**, 037103.

El, G. A., Grimshaw, R. H. J. & Smyth, N. F. 2006 Unsteady undular bores in fully nonlinear shallow-water theory. *Phys. Fluids* **18**, 027104.

El, G. A., Grimshaw, R. H. J. & Smyth, N. F. 2008 Asymptotic description of solitary wave trains in fully nonlinear shallow-water theory. *Physica* D **237**, 2423–2435.

El, G. A., Khodorovskii, V. V. & Tyurina, A. V. 2005 Undular bore transition in bi-directional conservative wave dynamics. *Physica* D **206**, 232–251.

Ertekin, R. C., Webster, W. C. & Wehausen, J. V. 1986 Waves caused by a moving disturbance in a shallow channel of finite width. *J. Fluid Mech.* **169**, 275–292.

Fornberg, B. & Whitham, G. B. 1978 A numerical and theoretical study of certain nonlinear wave phenomena. *Phil. Trans. R. Soc. Lond.* **289**, 373–404.

Gavrilyuk, S. L. 1994 Large amplitude oscillations and their "thermodynamics" for continua with "memory". *Eur. J. Mech.* B/*Fluids* **13**, 753–764.

Gobbi, M. F., Kirby, J. T. & Wei, G. 2000 A fully nonlinear Boussinesq model for surface waves. Part 2. Extension to o(kh)4. *J. Fluid Mech.* **405**, 181–210.

Green, A. E. & Naghdi, P. M. 1976 A derivation of equations for wave propagation in water of variable depth. *J. Fluid Mech.* **78**, 237–246.

Grimshaw, R. H. J. & Smyth, N. F. 1986 Resonant flow of a stratified fluid over topography. *J. Fluid Mech.* **169**, 429–464.

Grimshaw, R. H. J., Zhang, D. H. & Chow, K. W. 2007 Generation of solitary waves by transcritical flow over a step. *J. Fluid Mech.* **587**, 235–354.

Gurevich, A. V. & Pitaevskii, L. P. 1974 Nonstationary structure of a collisionless shock wave. *Sov. Phys. JETP* **38**, 291–297.

Johnson, R. S. 2002 Camassa–Holm, Korteweg–de Vries and related models for water waves. *J. Fluid Mech.* **455**, 63–82.

Kim, J. W., Bai, K. J., Ertekin, R. C. & Webster, W. C. 2001 A derivation of the Green–Naghdi equations for irrotational flow. *J. Engng Math.* **40**, 17–24.

Lamb, K. G. & Yan, L. 1996 The evolution of internal wave undular bores: comparison of a fully nonlinear numerical model with weakly nonlinear theory. *J. Phys. Oceanogr.* **26**, 2712–2734.

Madsen, P. A., Bingham, H. B. & Schäffer, H. A. 2003 Boussinesq-type formulations for fully nonlinear and extremely dispersive water waves: derivation and analysis. *Proc. R. Soc. Lond.* A **459**, 1075–1104.

Mei, C. C. 1983 *The Applied Dynamics of Ocean Surface Waves*. Wiley and Sons.

Miles, J. W. & Salmon, R. 1985 Weakly dispersive nonlinear gravity waves. *J. Fluid Mech.* **157**, 519–531.

Nadiga, T., Margolin, L. G. & Smolarkiewicz, P. K. 1996 Different approximations of shallow fluid flow over an obstacle. *Phys. Fluids* **8**, 2066–2077.

Smyth, N. F. 1987 Modulation theory for resonant flow over topography. *Proc. R. Soc. Lond.* A **409**, 79–97.

Su, C. H. & Gardner, C. S. 1969 Korteweg–de Vries equation and generalisations III. Derivation of the Kortwewg–de Vries equation and Burgers equation. *J. Math. Phys.* **10**, 536–539.

Tyurina, A. V. & El, G. A. 1999 Hydrodynamics of modulated finite-amplitude waves in dispersive media. *J. Exp. Theor. Phys.* **88**, 615–625.

Whitham, G. B. 1974 *Linear and Nonlinear Waves*. Wiley and Sons.